Journal of Physics: Conference Series **551** (2014) 012034 doi:10.1088/1742-6596/551/1/012034

β-detected nuclear quadrupole resonance and relaxation of $^8Li^+$ in sapphire

Z Salman[1], K H Chow[2], M D Hossain[3], R F Kiefl[3,4], C D P Levy[4], T J Parolin[5], M R Pearson[4], H Saadaoui[1], D Wang[3] and W A MacFarlane[5]

[1] Laboratory for Muon Spin Spectroscopy, Paul Scherrer Institute, CH-5232 Villigen PSI, Switzerland
[2] Department of Physics, University of Alberta, Edmonton T6G 2G7, AB, Canada
[3] Department of Physics and Astronomy, University of British Columbia, Vancouver V6T 1Z1, BC, Canada
[4] TRIUMF, 4004 Wesbrook Mall, Vancouver V6T 2A3, BC, Canada
[5] Department of Chemistry, University of British Columbia, Vancouver V6T 1Z1, BC, Canada

E-mail: zaher.salman@psi.ch

Abstract. We report detailed behaviour of low energy ^{8}Li implanted near the surface of α-Al_2O_3 single crystal, as revealed by beta-detected NQR of ^{8}Li. We find that the implanted ^{8}Li occupies at least two sites with non-cubic symmetry in the Al_2O_3 lattice. In both sites the ^{8}Li experiences axially symmetric electric field gradient, with the main principal axis along the c-crystallographic direction. The temperature and field dependence of the spin lattice relaxation of ^{8}Li in α-Al_2O_3, indicate that the ^{8}Li diffusion is negligible on the scale of its lifetime, 1.21 s.

1. Introduction

Sapphire (α-Al_2O_3) is an important material with many technological applications, for example in optoelectronics, catalysis and environmental chemistry [1]. It is an exceptionally stable oxide with a very large formation enthalpy, high mechanical strength and thermal conductivity, which is often used as a substrate for thin film deposition. Point defects can strongly modify the properties of sapphire, which may affect its use, for example in proposed gravity wave detectors [2]. Therefore, they are of considerable interest, and have been the subject of numerous theoretical investigations [3, 4, 5]. Ion implantation is an important method to create point defects in materials and thereby modify their properties as has been studied extensively in sapphire [6], including as a synthetic route to included metallic nanoparticles [7]. There are, however, few detailed investigations of the crystallographic sites of low dose and low energy implanted ions in the crystalline matrix [8, 6].

In addition to the importance of point defects, it has been shown that mixtures of sapphire with Li ionic conductor nanoparticles can enhance Li^+ conductivity in these materials [9, 10]. This effect was attributed to the heterointerface in this nanocomposite material. However, the contribution of sapphire to this enhancement and its microscopic details are still not well understood.

In this paper we present zero magnetic field β-detected nuclear quadrupole resonance (β-NQR) of $^8Li^+$ implanted near the surface of sapphire. We find that ^{8}Li occupies at least two

inequivalent crystallographic sites, distinguished by their local quadrupolar interactions. Both sites exhibit an axially symmetric electric field gradient (EFG), with the main principal axis (MPA) along the c-crystallographic direction. We also measure the temperature dependence of the resonance spectra and the spin lattice relaxation down to liquid helium temperatures. The temperature and field dependence of the spin lattice relaxation rate indicate that the main source of spin relaxation of ^{8}Li in Al_2O_3 is fluctuations of the EFG. These results rule out ^{8}Li diffusion in sapphire, even near its surface at and below 300 K.

2. Experimental

β-NQR is a magnetic resonance technique similar to nuclear magnetic resonance and muon spin relaxation (μSR). The local spin probe used in these experiments is ^{8}Li. A low energy (28 keV) beam of radioactive $^8Li^+$ is produced at the isotope separator and accelerator (ISAC) at TRIUMF in Vancouver, Canada. It is then spin-polarized using a collinear optical pumping method, yielding nuclear polarization as high as 70%, and subsequently implanted into the studied sample. Since the implanted beam energy is relatively low, the ^{8}Li stops near the surface of the sample, e.g. at an average depth of ~ 1500 Å in Al_2O_3 at the implantation energy used here. The nuclear polarization, and its time evolution, is the quantity of interest in our experiments. It can be measured through the β-decay asymmetry, where an electron is emitted preferentially opposite to the direction of the nuclear polarization at the time of decay [11] and detected by appropriately positioned scintillation counters. ^{8}Li is a spin $I = 2$ nucleus with a small electric quadrupole moment $Q = +31.4$ mB and gyromagnetic ratio $\gamma = 6.3015$ MHz/T. The magnetic resonance is detected by monitoring the time-averaged nuclear polarization as a function of a small radio frequency (RF) magnetic field applied perpendicular to the initial polarization direction. Alternatively, the spin lattice relaxation of the ^{8}Li nuclear spin can be measured by implanting a short pulse of beam (e.g. 4 seconds) and measuring the polarization as a function of time during and after the beam pulse with no RF field. More details about the technique can be found in Refs. [12, 13].

In the experiments reported here, the sample is an epitaxially polished single crystal substrate of α-Al_2O_3. The c-axis oriented crystal was 12.5mm square and 0.5 mm thick. It was mounted on the cold finger of a He flow cryostat. In all the measurements, the c-axis was oriented 45° relative to the Li nuclear polarization. The experiments were performed in zero and low magnetic field, applied along the initial nuclear polarization of the implanted ^{8}Li.

3. Theory

Typically, the implanted ^{8}Li resides at well-defined crystalline lattice sites which can be interstitial or substitutional. Sites with non-cubic symmetry are characterized by an EFG which couples to the electric quadrupole moment of ^{8}Li giving rise to a zero field (ZF) splitting in the nuclear spin levels [14]. This splitting and the resulting nuclear quadrupole resonance spectrum are thus a fingerprint of the ^{8}Li site. Assuming the EFG tensor is axially symmetric about z, the quadrupolar spin Hamiltonian is [15]:

$$H_q = h\nu_q[I_z^2 - 2] \tag{1}$$

where $\nu_q = e^2qQ/8$, $eq = V_{zz}$ is the EFG along z, and Q is the electric quadrupole moment of the nucleus. The energy eigenvalues, $E_m = h\nu_q(m^2 - 2)$, are a function of the azimuthal quantum number m where $I_z|m\rangle = m|m\rangle$. Small perturbations, such as small magnetic fields or slight deviations in the quadrupolar interaction, can have a surprisingly large effect on the nuclear polarization and β-NQR measurements. This may be traced to the fact that in zero magnetic field the $|\pm m\rangle$ states are degenerate and therefore easily mixed by small perturbations. Crystal imperfections, resulting in, for example, non-axial terms in the EFG, also lead to $|\pm m\rangle$ state

mixing. Consider for example a small term which breaks the axial symmetry of the EFG [14, 16]:

$$H_\eta = \eta h \nu_q (I_x^2 - I_y^2). \tag{2}$$

Here η is the conventional dimensionless EFG asymmetry parameter [14, 16]. H_η mixes the $m = \pm 1$ levels in first order with a characteristic frequency splitting between the mixed levels. We have shown [13, 17] that even small values of η (e.g. 0.01) will produce strong mixing of the $|\pm m\rangle$ states and a resulting fast drop of the initial nuclear polarization. Therefore, our β-NQR measurements are effectively insensitive to ^{8}Li sites with non-axial EFG, such as sites near a defect or vacancy. In what follows we will assume $\eta = 0$.

Another perturbation that can lead to mixing between different $|m\rangle$ states is a small magnetic field perpendicular to z (the MPA). Consider first a small magnetic field which is oriented along z, $\mathbf{B} = B\hat{z}$. The resulting Zeeman interaction lifts the degeneracy between $|\pm m\rangle$ states in first order but does not mix the states since it commutes with H_q. Although the measured resonance positions are shifted by a small amount there is no change in the amplitudes. For example, the resonance corresponding to the $|2\rangle \rightarrow |1\rangle$ transition shifts by γB. On the other hand if $\mathbf{B} = B\hat{x}$ is applied in the x direction the Zeeman interaction does not commute with H_q. Such a perturbation mixes the different m levels and consequently has a dramatic effect on the nuclear polarization. In general, the Hamiltonian of the ^{8}Li spin in an applied field $\mathbf{B}$ is

$$H = H_q - h\nu \left(I_z \cos\theta + I_x \sin\theta \right), \tag{3}$$

where $\nu = \gamma B$ and θ is the angle between the MPA and the applied field direction. Using perturbation theory the dimensionless mixing $\Delta_{m,n}$ between states $|m\rangle$ and $|n\rangle$ can be written as (see e.g. [13])

$$\begin{aligned}
\Delta_{2,1} &= \left(\frac{\nu \sin\theta}{3\nu_q - \nu\cos\theta}\right)^2 \simeq \frac{\sin^2\theta}{9}\left(\frac{\nu}{\nu_q}\right)^2 \\
\Delta_{-2,-1} &= \left(\frac{\nu \sin\theta}{3\nu_q + \nu\cos\theta}\right)^2 \simeq \frac{\sin^2\theta}{9}\left(\frac{\nu}{\nu_q}\right)^2 \\
\Delta_{1,0} &= \frac{3}{2}\left(\frac{\nu \sin\theta}{\nu_q - \nu\cos\theta}\right)^2 \simeq \frac{3\sin^2\theta}{2}\left(\frac{\nu}{\nu_q}\right)^2 \\
\Delta_{-1,0} &= \frac{3}{2}\left(\frac{\nu \sin\theta}{\nu_q + \nu\cos\theta}\right)^2 \simeq \frac{3\sin^2\theta}{2}\left(\frac{\nu}{\nu_q}\right)^2 .
\end{aligned} \tag{4}$$

Note that $\Delta_{m,n}$ for all other m and n values vanish in first order. Provided this mixing is larger or comparable to the ^{8}Li decay rate, it will affect both the measured initial nuclear polarization and its relaxation rate.

4. Results

In the process of carrying out the resonance measurements, we found that the $^8Li^+$ beam caused the sapphire crystal to scintillate (see Fig. 1), likely due to the β-emission produced in its decay

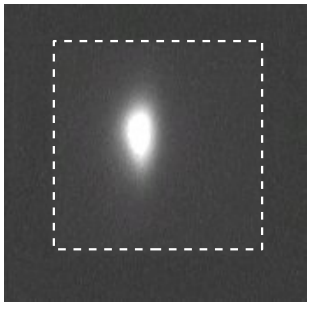

Figure 1. Demonstration of sapphire's use as a scintillator. The image of the $^8Li^+$ beam impinging on sapphire at a rate of 10^7 per second, taken with a CCD camera over a 10 second exposure. The dashed line highlights a 8x8 mm^2 area.

as well as the subsequent α decay of its daughter ^{8}Be. This property is not surprising in

view of sapphire's well-known luminescent properties [18, 19], but it does provide an interesting application as an ultra-high vacuum compatible, thermally conductive backing material for β-NMR samples, which enables tracking and positioning of the beam accurately on small samples.

Initially we tried to measure β-NQR spectra, while implanting ^{8}Li with its polarization perpendicular to the c-axis of the Al_2O_3 crystal. Under these conditions there was no measurable asymmetry in ZF, possibly due to (i) all the implanted ^{8}Li occupy a site with a very small nuclear quadrupole interaction, (ii) the MPA at ^{8}Li site is along the c-axis, or (iii) a large η which produces a large mixing between the different $|m\rangle$ states and a subsequent loss of polarization. However, when we rotated the Al_2O_3 crystal by 45°, two resonances were observed at room temperature with a non-vanishing asymmetry off resonance (Fig. 2). This clearly indicates that

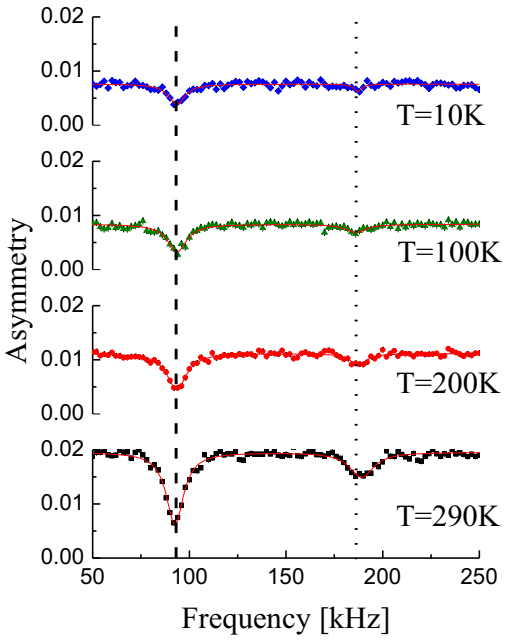

Figure 2. β-NQR spectra at various temperatures and in ZF. There is no significant temperature dependence of the resonance frequency, amplitude or broadening. Note however, a reduction of the baseline asymmetry is observed as the temperature is lowered. The solid lines are fits to Lorentzian lineshapes.

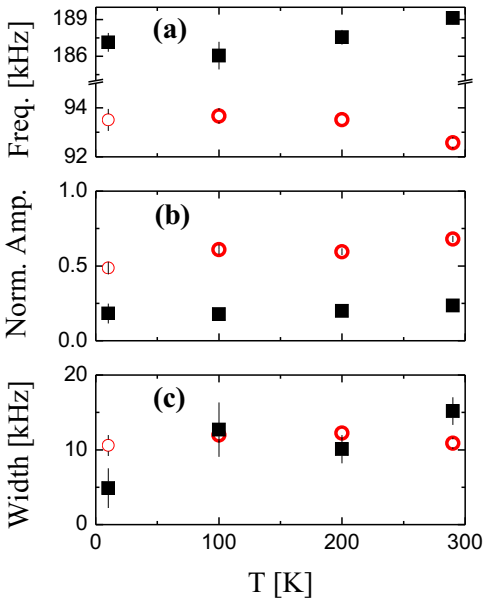

Figure 3. The resonance frequencies (a), normalized amplitudes (b) and widths (c) as a function of temperature, obtained from fitting the β-NQR spectra to Lorentzian lineshapes. The circles and squares indicate low and high frequency resonance parameters, respectively.

at least a large fraction of the ^{8}Li occupy sites with a nearly axial EFG which is oriented along the c-axis. The two resonances are attributed to two distinct sites, each with a different EFG tensor. Since the ratio between the resonance frequencies of the two lines is ~ 2, they cannot be attributed to the $|\pm 2\rangle \rightarrow |\pm 1\rangle$ and $|\pm 1\rangle \rightarrow |\pm 0\rangle$ transitions which should have a ratio of 3 in ZF. As can be seen in Figs. 2 and 3, there is no significant temperature dependent shift or broadening of the resonances, such as that seen in the β-NQR signal in $SrTiO_3$[17]. However, the measured asymmetry off resonance (i.e. the baseline of the spectra) decreases by 50% from 290 K down to 10K. This decrease can be attributed to an increase in the spin lattice relaxation of ^{8}Li as the temperature is decreased (see below).

The observed resonances fit very well to Lorentzian lineshapes. From these fits we extract

the resonance frequencies, their amplitudes (normalized by the baseline), and widths as shown in Fig. 3. The first resonance frequency is between 92-94 kHz while the second falls between 186-189 kHz, with corresponding normalized amplitudes of ~ 0.6 and ~ 0.2 and an almost equal width of ~ 10 kHz. We do not observe a strong temperature dependence, indicating that there are no sudden changes in the structural/electronic properties of sapphire or of the $^8Li^+$ site. The small variations as a function of temperature could be due to thermal expansion/contraction. Note that the sum of normalized amplitudes is ~ 0.8 leaving a possibility that a small fraction of ^{8}Li is implanted in sites with nearly cubic symmetry or non-axially symmetric EFG.

Now we turn to the discussion of the spin lattice relaxation of the ^{8}Li nuclear polarization. As mentioned earlier, this is measured by implanting the ^{8}Li beam for a period of 4 seconds, and measuring the polarization as a function of time, $p_z(t)$, during and after the beam pulse. Typical polarization curves measured at various temperatures in ZF are shown in Fig. 4(a). Note the gradual increase of the relaxation rate as the temperature is decreased. In contrast,

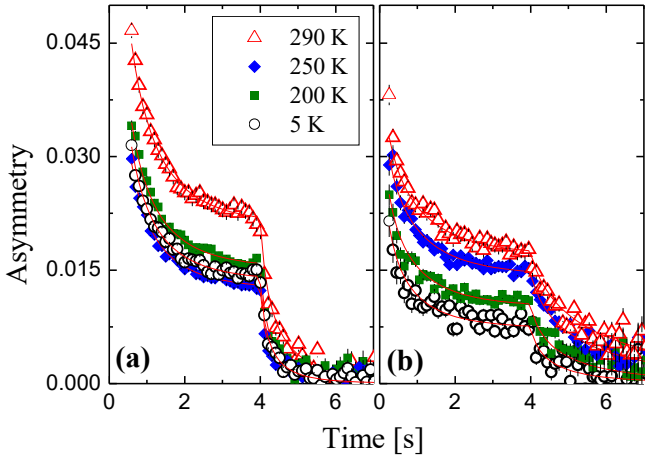

Figure 4. $p_z(t)$ measured in (a) ZF and and (b) 15 mT at various temperatures. The angle between the c-axis of the Al_2O_3 crystal and the initial polarization is 45°. The solid lines are fits to stretch exponential relaxation function (see text).

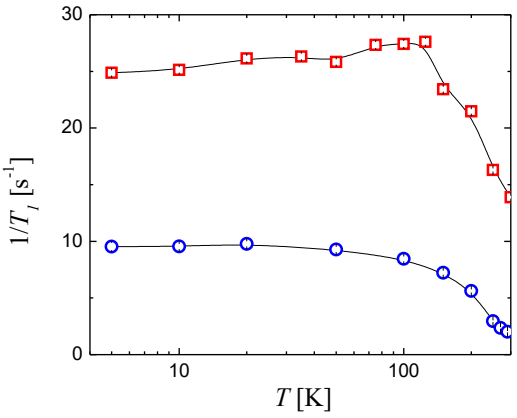

Figure 5. The temperature dependence of the spin lattice relaxation rate as a function of temperature at zero field (circles) and at 15 mT (squares). The solid lines are a guide for the eye.

measurements of $p_z(t)$ in a magnetic field of 15 mT, applied along the direction of the ^{8}Li initial nuclear spin, show that in this case the relaxation rate does not increase monotonically with decreasing temperature [Fig. 4(b)]. Rather, it peaks at ~ 125 K and then decreases gradually as the temperature is decreased further. $p_z(t)$ in these measurements is determined by both the ^{8}Li spin-lattice relaxation rate $1/T_1$ and its radioactive lifetime $\tau = 1.21$s. Assuming a general spin relaxation function $f(t, t_p : 1/T_1)$ for the fraction of ^{8}Li implanted in the sample at t_p, the polarization follows [17]

$$p_z(t) = \begin{cases} \dfrac{\int_0^t e^{-(t-t_p)/\tau} f(t,t_p{:}1/T_1) dt_p}{\int_0^t e^{-t/\tau} dt} & t \le T \\ \dfrac{\int_0^T e^{-(T-t_p)/\tau} f(t,t_p{:}1/T_1) dt_p}{\int_0^T e^{-t/\tau} dt} & t > T. \end{cases} \quad (5)$$

The data in Figs. 4(a) and (b) were fit to Eq. (5) with a phenomenological stretch exponential form,

$$f(t, t_p : 1/T_1) = A_0 e^{-[(t-t_p)/T_1]^\beta}. \quad (6)$$

In the fits we assume that the initial asymmetry, A_0 (which is proportional to the initial polarization), and the exponent β are common for all temperatures, which yields $A_0 = 0.53(6)$ in ZF and 0.200(6) in 15 mT with $\beta = 0.43(2)$ for both fields. The relaxation rates obtained from the fits are shown in Fig. 5. As expected, $1/T_1$ in ZF increases gradually below 290 K and saturates below 100 K, while in 15 mT it increases sharply below 290 K, peaks at ~ 125 K and then decreases gradually as temperature is decreased further. Note, in the 15 mT measurements the applied field enhances the relaxation rate. This is due to mixing, $\Delta_{m,n}$, between the $|m\rangle$ and $|n\rangle$ states produced by the magnetic field component, B_x perpendicular to the MPA of the EFG. The effect of the applied field on the relaxation may also be responsible for the difference in the temperature dependence of the relaxation rate between the ZF and 15 mT measurements. We should also point out here that the measured $1/T_1$ in this case reflects the weighted average of the $1/T_1$ of both sites.

5. Conclusions

The stopping site of ^{8}Li is consistent with the results from channelling experiments on Er implanted sapphire [8]. There it was found that at room temperature $\sim 70\%$ of the Er occupy an interstitial site near the free octahedral site while $\sim 20\%$ occupy the tetrahedral site. Both sites exhibit an axially symmetric EFG, with the MPA along the c-crystallographic direction. The temperature dependence of $1/T_1$ resembles that of the lattice constants in sapphire [20]. This is strong indication that the main source of spin relaxation of ^{8}Li in Al_2O_3 is small fluctuations of the EFG, which also scale with the lattice constants. These results rule out ^{8}Li diffusion in sapphire, even near its surface, as a contributor to the enhanced Li conductivity in mixtures of sapphire with Li ionic conductor nanoparticles [9, 10] .

Acknowledgments

We acknowledge the technical assistance of R. Abasalti, B. Hitti, D. Arseneau, S. Daviel, and funding from NSERC Canada. TRIUMF is funded in part by NRC Canada.

References

[1] Al-Abadleh H and Grassian V 2003 *Surf. Sci. Rep.* **52** 63
[2] Yan Z *et al.* 2004 *J. Opt. A* **6** 635
[3] Jacobs P W M and Kotomin E A 1994 *J. Am. Ceram. Soc.* **77** 2505–2508
[4] Jacobs P W M and Kotomin E A 1992 *Phys. Rev. Lett.* **69** 1411
[5] Carrasco J, Gomes J R B and Illas F 2004 *Phys. Rev.* B **69** 064116
[6] McHargue C J 1998 *Mat. Sci. Eng. A* **253** 94–105
[7] Stepanov A L and Khaibullin I B 2005 *Rev. Adv. Mater. Sci.* **9** 109129
[8] Alves E, daSilva M F, vandenHoven G N, Polman A, Melo A A and Soares J C 1995 *Nucl. Instrum. Meth.* B **106** 429–432
[9] Ardel G, Golodnitsky D, Peled E, Wang Y F, Wang G, Bajue S and Greenbaum S 1998 *Solid State Ionics* **115** 477–485
[10] Wilkening M, Indris S and Heitjans P 2003 *Phys. Chem. Chem. Phys.* **5** 2225–2231
[11] Crane S G, Brice S J, Goldschmidt A, Guckert R, Hime A, Kitten J J, Vieira D J and Zhao X 2001 *Phys. Rev. Lett.* **86** 2967
[12] Morris G D, MacFarlane W A, Chow K H, Salman Z, Arseneau D J, Daviel S, Hatakeyama A, Kreitzman S R, Levy C D P, Poutissou R, Heffner R H, Elenewski J E, Greene L H and Kiefl R F 2004 *Phys. Rev. Lett.* **93** 157601
[13] Salman Z, Reynard E P, MacFarlane W A, Chow K H, Chakhalian J, Kreitzman S R, Daviel S, Levy C D P, Poutissou R and Kiefl R F 2004 *Phys. Rev.* B **70** 104404
[14] Cohen M and Reif F 1957 *Solid State Physics* **5** 321–438
[15] Slichter C P 1990 *Principles of Magnetic Resonance* 3rd ed (New York: Springer-Verlag)
[16] Das T and Hahn E L 1958 *Nuclear Quadrupole Resonance Spectroscopy* (Academic Press Inc.)
[17] Salman Z, Kiefl R F, Chow K H, Hossain M D, Keeler T A, Kreitzman S R, Levy C D P, Miller R I, Parolin T J, Pearson M R, Saadaoui H, Schultz J D, Smadella M, Wang D and MacFarlane W A 2006 *Phys. Rev. Lett.* **96** 147601

[18] Caulfield K J, Cooper R and Boas J F 1993 *Phys. Rev.* B **47** 55
[19] Kotomin E, Tale I, Butlers P and Kulis P 1989 *J. Phys. Cond. Mat.* **1** 6777–6785
[20] Lucht M, Lerche M, Wille H C, Shvyd'ko Y V, Rüter H D, Gerdau E and Becker P 2003 *J. Appl. Cryst.* **36** 1075–1081